NASA TECHNICAL MEMORANDUM

NASA TM X-52949

NASA TM X-52949

ELECTRON OPTICAL METALLOGRAPHIC INSTRUMENTS

by C. W. Andrews
Lewis Research Center
Cleveland, Ohio

ABSTRACT

Some principles, characteristics, applications, and limitations of the Electron Microprobe X-ray Analyzer (EMXA), the Scanning Electron Microscope (SEM), and the conventional Transmission Electron Microscope (TEM) are outlined. The EMXA is emphasized due to its practical power and versatility. The various modes of operation available, and a normal sequence of steps in the analysis of a completely unknown sample are described. Some advantages and limitations of various microprobe intensity correction procedures, and of computerized correction calculations are given. Examples of microprobe and SEM applications are given.

E-6106

ELECTRON OPTICAL METALLOGRAPHIC INSTRUMENTS

by C. W. Andrews

Lewis Research Center

SUMMARY

Three electron-optical metallographic instruments are described: the Electron Microprobe X-ray Analyzer (EMXA), the Scanning Electron Microscope (SEM), and the conventional Transmission Electron Microscope (TEM). The purpose is to acquaint materials technologists with their important characteristics and their similarities and differences, and particularly to point out their capabilities and limitations.

Most attention is devoted to the microprobe, as a result of its ability to provide a wide range of analytical information unavailable by other techniques. Its capabilities include scanning electron microscopy as well as chemical analysis of solid surfaces by characteristic X-ray emissions. Scanning electron microscopy is available with the EMXA at some sacrifice in resolution and versatility relative to an actual Scanning Electron Microscope. The Transmission Electron Microscope is described only sufficiently to place its capabilities and limitation in perspective relative to those of the microprobe and SEM.

As background, some of the unique capabilities of the Ion Probe Mass Spectrometer Analyzer (IPMSA) are mentioned briefly. This instrument can analyze all elements, even discriminating among the isotopes of each, has lower limits of detectability than the EMXA, and can by ion sputtering bore into a surface to provide analyses versus depth.

The desirability of buying service on one of these very expensive instruments before purchasing it is pointed out. The main components of a microprobe are described in terms of their analogue equivalents: the X-ray tube, the TEM, and the X-ray fluorescence analyzer.

Functional modes of the microprobe are described by presenting a stepwise approach to the analysis of an unknown sample, starting with the

E-6106

backscatter-electron raster micrograph, followed by the spectral scan, then X-ray raster micrographs, and finally continuous or step traverses of the sample to develop concentration profiles. Shortcomings of computer calculations are indicated. Illustrations of applications of the EMXA and the SEM are given.

ELECTRON-OPTICAL EQUIPMENT AND TECHNIQUES

Introduction

Some principles and applications of three electron-optical instruments are summarized here: The Electron Microprobe X-ray Analyzer (Microprobe, or EMXA), the Scanning Electron Microscope (SEM), and the conventional Transmission Electron Microscope (TEM). The microprobe is emphasized because it is the most versatile and useful of the three for the practically oriented metallographic laboratory, and because a description of it also will have described most of the basic features of the SEM. Discussion of the TEM will be limited to a few comments to help place it and its applications in proper perspective relative to the microprobe and SEM. The TEM has been a commercial laboratory instrument much longer than the microprobe and SEM, and therefore most materials technologists have at least some familiarity with it.

Before entering upon the main subject, brief mention should be made of a powerful "relative" of the microprobe: the ion-probe mass-spectrometer analyzer. This is barely commercially available, and has not yet evolved to a common basic configuration as has the electron microprobe. It can analyze all elements, including the lower-atomic-number elements which can be analyzed only with difficulty or not at all by the microprobe. Its limits of detection (ppm to ppb) generally are much lower than those of the electron microprobe, especially for light elements. It can strip off successive layers of atoms from a sample by ion sputtering, providing analyses versus depth (i.e., in three dimensions). It also analyzes separately each isotope of an element and each ionizable molecular fragment. In fact, one of its disadvantages may

be that the finely detailed output of the ion-beam instrument can necessitate time-consuming reorganization of the data into meaningful form. It might be necessary, for example, to obtain the total iron concentration in a sample by summing its components appearing in the mass-charge spectrum as divalent and trivalent ions, as ions of the several isotopes, and as a series of complex ions.

Other related electron-optical instruments exist which presently are more limited in availability and range of application than the microprobe, SEM, and TEM. They include the mirror electron microscope, the ultraviolet-stimulated-emission electron microscope, and specialized versions of the microprobe and SEM, as well as various hybrids of the microprobe, SEM, and/or TEM.

This discussion may indirectly suggest important applications of these instruments to materials problems. Caution is in order, for they are expensive to buy, operate and maintain. Dedicated attention of one or more skilled operators is required. Depreciation is very high, since initial cost may be $50,000 to $150,000, and a current model is likely to be obsolete in four to eight years.

Therefore, it is advisable to purchase instrument and operator time from a commercial laboratory first. SEM and microprobe service now is available from a number of nationally reputable organizations. One should select a service source carefully, then, if possible, be present to watch at least some part of the instrument operation on his sample, at least during the first few sample submissions. Close liaison is extremely important to the service organization's success in providing the information the requester needs, and to the latter's success in interpreting that information. Some idea of costs is provided by the price for SEM service of $500 per day quoted by one reputable commercial laboratory.

Electron Microprobe X-ray Analyzer

Outline of main components and features. - A typical microprobe with one

crystal spectrometer is shown diagrammatically in figure 1. It may be considered as a combination of portions of an X-ray tube, a conventional electron microscope, and an X-ray fluorescence analyzer. As in the X-ray tube, the microprobe has a hot filament which emits electrons, and a target to which electrons are accelerated through a high potential gradient. Here the sample is the target. As in the TEM, the electrons initially are focussed by a grid cap and anode plate, then additionally by two or more magnetic lenses, and the main accelerating potential is between filament and anode plate. The demagnified filament image formed by the electron beam on the sample surface (incident beam spot size) is less than a micron (0.000040 in.) in diameter. As in the X-ray fluorescence analyzer, characteristic X-rays are emitted from the sample (here excited by the incident electron beam) and are dispersed and detected by a focussing crystal spectrometer consisting of a diffracting crystal and a gas-proportional detector. Crystal and detector are movable through arcs on a focal circle which passes through the point of electron-beam incidence on the sample surface. The sample can be translated (X and Y) mechanically under the beam, or the beam can be translated (a lesser distance) electromagnetically across the sample surface. By means of scan generators, the beam also can be moved rapidly in a television-raster pattern of adjustable size on the sample, not over a few hundred microns across. At the same time, the spot of an oscilloscope display is moved in synchronism by the same scan signals in a raster usually 10 centimeters across. The display intensity is modulated by selected electron or X-ray signals excited in the sample surface by the incident electron beam as it sweeps out its raster. The result is a magnified picture on the display tube face of the scanned area of the specimen in which brightness is proportional to concentration of a selected element, or in the case of electron signals, to topographical features or average atomic number of the sample surface. The oscilloscope image is recorded photographically, and the resulting X-ray or electron raster micrographs provide very valuable metallographic information. However, the micrographs can be subject to serious misinterpretation in the hands of one not thoroughly familiar with the X-ray phenomena involved, as will be demonstrated later. When it is displaying the secondary-electron signal from the horizontal detector just below

and to the left of the sample in figure 1, the microprobe is operating as a scanning electron microscope.

Interactions between electron beam and atoms of sample surface. - Figure 2 summarizes some interactions of the incident-beam electrons with atoms in the sample surface. Most of the incident energy is converted into the following forms, approximately in order of decreasing relative quantity:

Heat into the sample
Sample current
Backscattered electrons
Secondary electrons
Characteristic and continuum X-rays
Auger electrons
Fluorescent light (some materials)
Diffracted X-rays, semiconductor effects, etc.

Note the concentric semicircles which represent schematically the relative shape and size of the regions involved.

These eight energy forms and their significance in microprobe analysis are summarized here in the order given above.

1. Heating of the sample is the major final result of most of the other interactions, and forms the basis of electron-beam welding.

2. Current between the sample and ground results from accumulation of electrons from the primary beam in the sample. It varies with both surface topography and average atomic number of the beam-excited region in the sample surface. It is possible to insert an amplifier input between the insulated sample and ground. The amplifier output then can be monitored in various ways to provide topographical or compositional information about the sample.

3. Backscattered electrons (BSE) have energies close to that of the incident beam, and so can emerge from well below the sample surface. They travel in straight trajectories from the sample surface, and their yield is sensitive to average atomic number, as well as to grosser surface topography. The BSE signal varies approximately inversely as the sample-current (SC) signal. However, the sample-current amplifier output may be reversed to bring it into phase with the BSE signal.

4. Secondary electrons have much lower energies, of the order of 50 electron volts or less, so that only those generated very close to the surface can escape and be detected. Therefore, their yield is sensitive mainly to surface topography. They often are drawn to the detector along curved trajectories by a positive bias of from 200 to greater than 2,000 volts. (Secondary-electron (SE) raster micrographs form the main disply mode of the SEM.)

5. X-rays excited by the electron beam include both background (continuum, or white) radiation and characteristic radiation. The background contains no analytical information. Characteristic radiation consists of several sharp peaks for each element, each at a precise, characteristic wavelength. For constant operating conditions, the peak height above background definitely is related to concentration in the sample of the element emitting that particular X-ray wavelength so that this radiation provides the real semiquantitative to quantitative analytical information. The relative amount of characteristic X-ray energy is small as suggested by its position in the preceding enumeration so that detection and counting statistics are constant problems with the small acceptance angles and low efficiencies of diffracting crystal spectrometers. X-ray output also can be displayed in the raster-micrograph mode, as well as in other modes to be outlined later.

6. Auger electrons have energies slightly greater than the 50-electron-volt upper limit of secondary electrons, and exhibit definite energy peaks characteristic of the elements emitting them. They therefore contain analytical information concerning the extreme outer surface layers of atoms of the sample. However, the peaks are so weak that electronic differentiation must be used to distinguish them. Techniques and interpretation are very sophisticated. The shallow "penetration" makes results extremely sensitive to surface-contamination effects; hence, most applications of Auger analysis occur in the complex field of surface chemistry. Auger analysis is not yet considered a practical tool for most applied metallographic laboratories.

7. Light fluorescence in some nonmetallic materials excited by the electron beam is useful in recognizing known types of inclusions, and in ascertaining whether specific elements identified in segregates by X-ray micrographs are present as oxides or other known light-fluorescing compounds. Color and intensity of fluorescence are the criteria but since these often are very sensitive to certain impurities in the parts-per-million range, they are at best very rough guides.

8. Diffracted X-rays and semiconductor effects are not generally used in practical microprobe analysis.

The "platform" in figure 2 under the incident beam represents the contamination spot, a kind of carbonaceous varnish from breakdown by the electron beam of organic molecules such as those of back-diffused pump oil. Its presence helps the analyst to know where the beam is on the sample, but it also has the disadvantage of greatly inflating the carbon X-ray intensity. It also somewhat decreases X-ray intensities from other elements present in the beam-excited region of the sample.

Characteristics of backscattered and absorbed (sample-current) electrons. - The relative yield of backscattered electrons increases with increasing atomic number of the sample excited region, so that light and dark areas in the backscatter-raster micrographs represent regions in the sample of high and low average atomic number, respectively. The relationship is shown in figure 3. Backscattered electrons subtract from sample current so that the sample-current micrograph is approximately the negative of the backscatter micrograph for a given region. Backscatter-electron or sample-current raster micrographs of a flat, polished sample provide a preliminary look at microsegregation according to average atomic number, and suggest where in the sample the microprobe analyst should run X-ray spectral scans to determine specifically what elements are present. Also, backscattered electrons are not available for exciting characteristic fluorescent X-rays, and therefore must be accounted for subtractively in making the "atomic number correction," which is mentioned later in this review.

General nature of characteristic X-rays. - As the accelerating potential

of the electron beam incident on a given element in a solid target is gradually increased, white X-ray radiation which is continuous with wavelength first appears and increases in intensity. Then at specific potentials, various characteristic peaks emerge above this "background," and their intensity increases rapidly relative to the background. The potential at which each peak first emerges is called its critical excitation potential, E_c.

Figure 4 diagrams some of the important energy transitions of the atom producing these characteristic peaks. If an incident-beam electron ejects an inner-shell K electron from an atom, and an L-shell electron drops down to replace the missing K electron, a K-alpha X-ray photon is emitted. If an M-shell electron drops down, the emitted photon is K-beta radiation having slightly higher energy (shorter wavelength). If an L-shell electron is ejected (which can result from incident electrons having lower energy than that required to eject K-shell electrons), an M-shell electron drops into the vacated L level and a longer wavelength (i.e., lower energy) L characteristic peak is excited. The K-alpha event is more probable than the K-beta which involves a greater energy change; therefore, the K-alpha peak is the higher, i.e., the more intense with more counts per second. L and M radiation require progressively lower microprobe accelerating potentials (i.e., have smaller E_c) relative to K radiation. Figure 5 is a plot of E_c versus atomic number, and it is quite apparent that L or M radiation must be used for analysis of the higher-atomic-number; i.e., "heavier" elements, since maximum accelerating potentials of commercial microprobes range only from 30 to 50 kilovolts.

Use of lower accelerating potentials and of L or M X-ray peaks may be advantageous in other ways. Figure 6 demonstrates one such advantage: the improved ability to distinguish inclusions in an X-ray raster micrograph when the low-energy L lines of iron (Fe) and nickel (Ni) and 5 kilovolts accelerating potential are used, rather than the K lines and 20 kilovolts. Figure 7 also illustrates this, and, in addition, shows the effectiveness of the BSE raster micrograph (upper left) in delineating inclusions of low average atomic number (darker) in a higher-atomic-number (brighter) matrix. In the Fe and Ni X-ray raster micrographs of both figures, the higher energy 20-kilovolts

electrons penetrate the inclusions, and the Fe and Ni X-rays from the matrix beneath emerge through them with little attenuation, so that the inclusions are nearly invisible. Conversely, lack of penetration by the lower-energy electrons and softer Fe and Ni L X-rays causes the inclusions to be outlined clearly.

Sample preparation and operational modes of the microprobe. - The major electron-beam interactions with the sample and some useful characteristics of the resulting emitted radiations have been reviewed. A few notes and precautions on sample preparation and some important information output modes which are available with the microprobe are now considered. These are classified somewhat arbitrarily as qualitative, semiquantitative, and quantitative, and this is the normal order of attack on a completely unknown sample.

Sample preparation and standards. - A polished, unetched metallographic sample is assumed. If nonconductive surface layers such as oxides are to be studied in a cross section, the microprobe analyst usually will have coated the sample with a grounded conductive, edge-retaining hard layer before sectioning, mounting and polishing. Electroplating of copper or nickel, or electroless nickel plating often have been used. Otherwise, as the sample edge with the adjacent nonconducting mount material approaches the beam during a specimen traverse, the mount material accumulates electrons from the beam and becomes charged, repelling the beam back away from the edge. Then distance on the strip-chart record no longer corresponds to distance on the sample, and quantitative relationships between the two are lost. Also, if the sample contains large nonconductive phases or inclusions, vacuum evaporation of a layer of carbon, copper or other conductive material a few hundred Angstroms thick onto the surface of the sample after mounting and polishing may be necessary to avoid charging effects. Another precaution in sample preparation is avoiding use of polishing compounds containing elements which are desired in the analysis; for example, silicon carbide when carbon or silicon analysis is required. The compound may imbed in soft phases or crevices and will then falsely affect the results of the analysis.

In microprobe analysis, a "standard" normally is required for each element of interest. It consists of a mounted and polished high-purity "chip" of the element being analyzed or of an alloy or compound of known uniform analysis containing that element. For constant operating conditions, the ratio of net (peak minus background) X-ray intensity for the sample to the net intensity for the corresponding 100 percent (elemental) standard (called the net intensity ratio) is a measure of the weight fraction of that element in the sample. In semiquantitative analysis, the weight fraction of an element in the sample generally is considered equal to its net intensity ratio.

When the foregoing sample and standard requirements have been met, both are inserted into the sample chamber, the microprobe is pumped to vacuum (in the order of 10^{-5} torr), and the desired settings of accelerating potential, sample current, spectrometer crystals and angles, and output electronics are made.

Backscatter-electron raster micrographs. - Backscatter-electron raster micrographs often are obtained as a preliminary indication of presence and location of segregation as previously indicated. Results of BSE micrographs and other probe analyses sometimes provide unexpected surprises for the requester. An example is the BSE micrograph shown in figure 8. This is IN 100 nickel-base superalloy, diffusion coated with Al-Cr-Fe alloy and air oxidized at 1900° F (1040° C). The bright spots along the interface indicated presence of one or more heavy elements, and were subsequently found to contain thorium. Since thorium had not been involved in preparation of the alloy or the coating, no satisfactory explanation for its presence could be found. Much later, when the sample was repolished to obtain a better BSE micrograph, the bright spots were no longer seen. It is speculated that the thorium was deposited on the sample in this unusual distribution from a contaminated polishing cloth during a previous metallographic preparation. The probe analyst must take great care to avoid all possibilities of developing such false structures (artifacts). Very often, however, unexpected analytical results from the microprobe have proved to be true, revealing material mix-ups and other previously unrecognized problems.

When segregations such as the bright spots mentioned in the preceding paragraph are observed in the BSE micrograph, the next logical step is to position the electron beam successively on a segregate area, and on the matrix, and to obtain a complete "spectral scan" for each position. This can be done by motor driving one or more spectrometers through a sufficient range of diffracting angles to display on the recorder chart all elemental peaks the probe is capable of analyzing. Thus, though unexpected, peaks for thorium were found in the bright spots, but were not found in the "matrix." An illustrative spectral scan for TD-Nickel (2 percent ThO_2 in nickel) is shown in figure 9. The two thorium M peaks are indicated; all other peaks are various diffracting orders (i.e., values of n in the Bragg equation $n\lambda = 2d \sin \theta$) of nickel K-alpha and K-beta radiation. This particular spectral scan was made to verify that a metallographic sample exhibiting a peculiar etching response was indeed TD-Ni.

X-ray raster micrographs. - X-ray raster micrographs often form the next step in a progressive analysis. They provide the information required if (1) the requester wants to compare the distribution of specific elements with the phases seen in a light micrograph, or (2) the BSE micrographs and spectral scans have shown presence of segregations, and what elements are involved, and it now must be determined in detail how these elements are distributed. In the X-ray micrographs, each white dot represents an X-ray or noise event in the detector or electronics, and significance can be attached only to definite concentrations or depletions of white dots. Even then, variations in the dot density can result from differences in X-ray background, not related to presence or absence of the element for which the spectrometer is set.

An example of the X-ray background effect is shown in figure 10. This is a section of a solar cell, whose main components are a cadmium sulfide layer with a copper-grid electrode on one face, which together are sandwiched between two layers of Kapton plastic. The spectrometer was set for copper, and the copper grid bar is delineated clearly by the high density of white dots in the lower (X-ray-raster) micrograph. The upper micrograph is the corresponding BSE image. The cadmium sulfide layer also appears

to contain some copper, according to its higher dot density than that of the Kapton on each face of it. But this is not so, as shown by the three spectral scans through the Cu peak only ("mini-scans") at the left side of the figure. These were obtained on the copper grid bar, on the CdS layer and on the Kapton plastic. It is clear that the increased density of white dots for the CdS layer is due to a higher background only; there is no copper peak in the CdS mini-scan, but the background is higher than that for the Kapton.

With adequate peak-background data for various dot densities, X-ray raster micrographs may be considered semiquantitative.

Sample line traverses. - A sample line traverse is considered semiquantitative, but can be truly so only if background, atomic number, absorption, and fluorescence effects are at least considered. These all become important in a semiquantitative analysis generally only if elements of widely differing atomic number are included.

The solar-cell example given above illustrates the importance of both peak and background information to correct interpretation of X-ray raster micrographs. It is equally important for sample line traverse, as illustrated by figure 11, which is a sketch of microprobe traverse results which have been encountered in steel analyses. Here oxygen X-ray intensity was anomalously lower for an alumina inclusion than for the steel matrix. However, as shown by the spectral-peak sketches of this figure, most of the "oxygen" X-ray intensity on the steel matrix was background; the net (i.e., total peak height minus background) oxygen intensity for the steel matrix actually was low. The net oxygen intensity for the aluminum oxide inclusion was much higher, as it should have been.

In a line traverse each of one-to-several spectrometers is set to a desired X-ray peak for an element of interest, and its signal is fed through integrating output electronics to one of the pens of a multichannel recorder. The sample then is traversed along a desired path under the electron beam by a synchronous motor. Again, precautions are needed to avoid beam-deflection effects caused by specimen charge-up which may nullify the correspondence between position on the recorder chart and position on the sample.

A short spectral scan (mini-scan) through the characteristic X-ray peak being used for analysis of each element is needed to provide background-correction information for even semiquantitative analysis. The spectrometer is motor-driven through the angle for the characteristic peak, starting and ending far enough from the peak position to insure that on the recorder chart the background level is clearly evident on each side of the peak. This must be done on the standard sample for a given element, and on a position on the unknown sample where that element is present in a concentration approximating the average concentration to be studied. If the concentration of a given element varies widely in a sample (i.e., it is strongly segregated), mini-scans should be obtained at several positions in the sample, each corresponding to a significant level of concentration of that element. An example of a sample traverse record with supporting spectral-peak mini-scans is shown in figure 12 for a carburized 4619 steel. The peak scans are, left-to-right, Ni, C, and Fe.

The only corrections generally applied to the raw X-ray intensities (plotted in the chart record versus distance on the sample) are the preceding approximate peak and background information from the mini-scans through the pertinent spectral peaks on sample and standards. The X-ray intensity on the chart above background is assumed to vary linearly with concentration of the element in the sample, at least over small composition ranges. In practice, for each element, the probe analyst usually visually applies the approximate background correction to each significant level on the chart record, and makes appropriate correction notations on the chart. Instead of a pure standard, a known concentration of the element in the sample matrix often may be used advantageously as a standard. The decision of what standard to use - sample, elemental, or compound - requires much experience and must consider both the accuracy desired and the amount of microprobe time that can be justified.

Point analyses. - Quantitative electron microprobe analyses are based on digital readout of X-ray intensities, and therefore are obtained with both electron beam and specimen stationary during each fixed-time counting interval; that is, they are point analyses. By obtaining such analyses at a series of points at equal small increments along a line in the sample, one produces

nearly the equivalent of a continuous sample line traverse. This is referred to as a step traverse.

If the utmost in quantitative results is required, and wide variations in composition are encountered within a sample, it will be necessary to obtain peak and background counts for each point of the step traverse. This is tedious and costly, for at each step the count rate (X-ray intensity) must be obtained both on peak and at a background position of the spectrometer. Thus each active spectrometer must be changed from peak position to a background position (or vice versa) at each step. If the compositional variations are quite small or if a less precise result is tolerable, automatic step traversing with fixed spectrometer settings and automatic printout of intensities can be utilized. This can be accomplished in perhaps one-tenth the time required for the more precise results involving the spectrometer detuning and retuning at each step.

A diffusion profile obtained by the step-traversing technique is shown with the corresponding phase diagram in figure 13. The high spatial resolution of the microprobe enables it to record precisely the steep compositional gradients encountered at the diffusion-couple interface. This accounts for the close agreement between the microprobe composition profile discontinuity and the composition limits of the two-phase field in the accepted gold-nickel phase diagram at the diffusion temperature used (750° C).

The probe analyst also can obtain individual point analyses at manually selected positions in the sample surface, in which case he initiates counting and data-transfer operations manually.

Hand calculation of corrected concentrations from raw intensity data, using graphical and slide rule or desk calculator methods, is possible in simple systems, with suitable standards. However, as the number of elements per analysis increases beyond two, this rapidly becomes excessively time-consuming and costly. Use of intermediate standards close to the unknown compositions, in combination with linear interpolation, is attractive for accuracy and ease of calculation, and is the only approach if a digital computer of sufficiently large core memory is not available. However, preparation of the many standards required can rapidly become an overwhelming task.

One cannot emphasize too strongly that even computer-calculated concentrations, using pure-element or compound standards, are no better than the largely empirical equations and the experimental constants used. Both equations and constants leave much to be desired in the present state of the art, especially when light and heavy elements occur together. Thus, computer-corrected microprobe analyses may and often do disagree substantially from established bulk analyses of the same material by conventional chemical techniques.

Corrections for Quantitative Microprobe Analyses

Whatever calculated-correction equations are used, there are six corrections which generally are applied to the raw X-ray intensity data. They are:

1. Instrumental drift
2. Deadtime
3. Background
4. Atomic number
5. Absorption
6. Fluorescence

The first three are single-calculation corrections which do not require the high-speed iterative capacity of a computer.

1. Instrumental drift is concerned with gradual changes with time in incident beam current, accelerating potential, amplifier stability, etc. Since the changes usually are linear with time, one needs only initial and final values for the analysis period, of count rates on pure standards. Corrected values for each analysis (i.e., each point of a step traverse) then are obtained by simple time-proportioning.

2. Deadtime is the recovery time of the detector tube between one entering X-ray quantum and the next, for full counting. It becomes significant for modern gas-proportional tubes only above several tens of thousand counts per second, and the correction is calculated readily.

3. Background corrections for individual point analyses may be obtained on the sample using a spectral mini-scan to show where true background is encountered on each side of the peak, then recording and averaging the background counts from these two positions. This average then is subtracted from the peak count at the same and similar points on the sample. Some features of this procedure were outlined here in the preceding section.

Corrections 4 through 6, atomic number, absorption, and fluorescence, require the composition of the incident-beam-excited region as input information. Initially, of course, this information is not available; therefore, the raw intensity ratios are used as first approximations, and the correction calculations are made. The resulting second-approximation composition is used as input for a second iteration of the calculation, and an improved third-approximation composition results. Using this, a third iteration is performed, and so on, until the difference between the results of the iteration just performed and the preceding one is less than some predetermined value.

4. The atomic number correction accounts for differences in electron stopping power and backscatter between the unknown sample (or different "characteristic" regions within the sample) and the standard. The phenomena involved are poorly understood, and "improved" equations continue to appear in the literature. As incident-beam electrons penetrate into the surface of the sample, they are scattered in all directions, and their energies are degraded by many types of interactions. With increasing depth and with increasing atomic number of the element being analyzed, fewer electrons have sufficient energy to excite K, L, or M characteristic X-rays of a given element and wavelength. Of those excited, only a fraction are directed backward toward the surface, and a substantial fraction of these will be absorbed in other interactions and will not emerge from the surface available for detection and measurement.

5. The absorption correction is intended to account for the attenuation of characteristic X-rays of the analyzed element, which are excited within the sample by the electron beam. Attenuation occurs during passage of the X-rays through the sample material from the point where they are generated, to the

surface where they can emerge and be detected. The correction usually will be large for detecting lesser concentrations of a light element in a heavy element matrix, and vice versa for the opposite combination (although there may be marked exceptions where fluorescence effects predominate). There also are discontinuous effects at X-ray absorption edges. Variables considered in the absorption correction include electron-beam accelerating potential, concentration of each element present, mass absorption coefficient of each element present for the characteristic wavelength being considered, X-ray takeoff angle of the microprobe, and average atomic weight and average atomic number of the excited region.

6. The fluorescence correction compensates for enhancement of the characteristic peak of the element being considered, by additional intensity excited in that element by higher-energy X-rays from other elements present in the excited volume of the sample. The fluorescence correction is not always significant, but this cannot be assumed and must be checked for a given alloy or series of similar alloys. The various fluorescence correction equations also are quite complex, including for exciting and/or excited elements such factors as ratio of absorption coefficients at the absorption edge, fluorescent yield, wavelength, atomic weights, and probe X-ray takeoff angle.

Size of Analyzed Volume in Sample

Spatial resolution of microprobe analysis, that is the size of the smallest region in a sample from which definite quantitative analytical information can be obtained, is not easy to determine. However, it is generally accepted that the region from which fluorescent X-rays are emitted and detected is several times larger in diameter than the incident beam spot, as suggested earlier by the diagram of figure 2. (Even the spot size for emission of backscatter electrons is on the order of twice the incident beam spot size.) This is shown quantitatively in figure 14, in which diameters of both backscatter-electron and characteristic-X-ray-emitting regions are plotted. A general rule-of-

thumb minimum diameter of the X-ray spot is 2 microns, and the upper curve appears to verify this. According to figure 14, as sample current is increased from 20 to 200 nanoamperes (nA), the minimum diameter of the incident beam spot almost doubles.

The 2-micron minimum X-ray diameter places a lower limit on the diameter and depth of a region such as an inclusion for which reliable analytical information can be obtained by the microprobe. If either dimension of an "inclusion" is less than this limit, X-ray intensities from the matrix as well as from the inclusion are likely to become part of the analysis. Of course, even if the inclusion meets or just slightly exceeds these minimum dimensions, it will tax the microprobe analyst's skill and patience to position the beam precisely at the center of it, and to maintain the beam there throughout the period of the analysis.

The versatility of the electron microprobe frequently has been extended to non-chemical-analysis applications. An example is shown in figure 15. These are calibration curves for 20 and 30 kilovolts accelerating potentials for measuring thickness of gold films. The gold L-alpha X-ray intensity increases almost linearly with increasing film thickness up to practical limits of electron and X-ray penetration. The film should be suspended, so that interfering X-rays cannot be excited in a substrate, or the substrate may be a low-atomic-number material such as beryllium, whose characteristic X-rays are too low in energy to cause interference.

SCANNING ELECTRON MICROSCOPE

Distinguishing Features of the SEM Relative to the Microprobe

Present commercial Scanning Electron Microscopes have depths of field several hundred times greater than the light microscope, and their resolution is about $1\frac{1}{2}$ orders of magnitude finer. This combination opens an entirely new realm of observation capabilities, from biological to geological, from manufacturing troubleshooting to crystal research.

Actually, the electron microprobe is in effect a scanning electron microscope when it is operating in the secondary-electron (SE) or backscatter-electron (BSE) raster-micrograph mode. The relative limitations of the probe here are (1) nearly tenfold poorer resolution, (2) less specimen maneuverability, especially tilting, which often is important for optimum image contrast, and (3) more rapid contamination and possibly damage of sample resulting from the higher beam current. Resolutions of 200 to 300 Angstroms are claimed for present-generation commercial SEM's. At least one probe manufacturer has now announced a lens modification to its instrument which is claimed to provide similar resolutions - an indication of the very fluid state of the art.

The SEM typically operates at sample currents three to four orders of magnitude less than those commonly used in microprobe analysis, with correspondingly smaller incident beam spot size - hence the better resolution and reduced contamination rate. The SEM also is more compact and simpler to operate than the probe. It provides primarily visual information, with spectacular depths of field and with useful magnifications from the order of 20X to about 20 000X.

However, a new dimension is opened for SEM's with recently developed solid-state X-ray detectors which collect X-rays very efficiently, have increasingly good energy resolution, and subtend a large solid angle at the sample surface. These are used in combination with a multichannel analyzer, to disperse the X-rays electronically according to their energies, and an oscilloscope display. Sometimes data also are recorded by a printout or magnetic tape.

Addition of this "energy X-ray analysis"(EXA) accessory endows the SEM with a unique range of chemical analysis capabilities, including some possessed by the electron microprobe, plus some beyond the capabilities of the conventional microprobe. An example of the latter is the ability to accumulate and display an entire X-ray spectrum simultaneously, at speeds nearly two orders of magnitude faster than the microprobe with its slow-acting crystal spectrometers. Another is the ability to "look at" (i.e., obtain X-ray spectra and X-ray micrographs from) rough or irregular surfaces such as fractures.

Useful X-ray count rates are possible even at the very low sample currents usually used in the SEM (10^{-11} to 10^{-12} A). The net result is much improved X-ray detection and counting efficiency, but at a sacrifice in light-element capability and in energy (or wavelength) resolution relative to crystal spectrometers. (Resolution here is the width of a displayed X-ray peak in electron volts (eV) at half-maximum height.)

The SEM with energy X-ray analysis has achieved breakthroughs such as localizing the segregation of specific elements within a single biological cell, thus completely altering certain metabolic theories. EXA also can be used with electron microprobes. In this application, the main benefits are ability to obtain analyses of irregular surfaces, greatly-increased speed of X-ray data acquisition, particularly spectral scans, and a substantial decrease in the required sample current, with the resulting benefits of smaller spot size and decreased contamination rate. While EXA presently is considered qualitative to semiquantitative, special computer programs and other techniques under development may soon render it quantitative.

Examples of SEM Applications

A few applications of the SEM will be presented, with emphasis on micrographs providing answers to practical problems. Figure 16 illustrates a recent and important troubleshooting use of the SEM for space hardware. The SERT II NASA-Lewis mission which was launched in February 1970 to test small ion thrusters almost did not fly due to plugging, cracking, and liquid-penetration of porous tungsten powder-metallurgy "mercury vaporizers." The fine structure and defects in these devices could be resolved satisfactorily only by the SEM. The required combination of resolution and depth of field was not available with light microscopy. Complete inspection of each of several vaporizers by examination of many contiguous fields such as the one shown here provided information essential to isolating and eliminating the faulty procedures leading to the malfunctions.

Another application is shown in figure 17. In a wide-spectrum "metallographic" laboratory, materials may be encountered which cannot be prepared and examined as polished samples. A case in point is this complex titanate under study for energy-conversion uses, which simply was too friable to withstand mounting and polishing. For SEM examination, it was necessary only to fracture the material, cement the fractured piece on to a sample block, and evaporate a gold-palladium conductive coating onto it to prevent beam charge-up. The resulting in-depth fractographs provided an adequate, though different, characterization of the structure, with minimum sample-preparation labor. Size, shape, and degree of bonding of the grains, as well as relative void volume are apparent.

More conventional polished and etched metallographic samples also can in some cases be examined advantageously in the SEM. Advantages here relative to the light microscope are increased useful magnifications and depth of field. However, atomic-number contrast, especially in the BSE mode, may also be useful. Figure 18 is an example of this application using the secondary electron display mode, showing an NiAl coating on IN 100 alloy, which has been oxidized in static air at 2000° F (1093° C) for 300 hours, then reheated and slow cooled. The Widmanstatten structure developed in the NiAl is revealed by electrolytic etching.

Extension of this philosophy of utilization of the SEM promises to open a new realm of metallographic techniques, using selective deep-etching to reveal structures in strong relief which could not be examined in the light microscope due to its very limited depth of field. Sample preparation can be simplified, since usually it is necessary only to grind through fine abrasive papers to provide an adequate surface. Final polishing steps can be eliminated. The deep etching apparently removes sufficient damaged surface material to reveal a true structure.

Silicon carbide crystals which have potential as high-temperature semiconductors, may occur in several crystallographic modifications depending on the complex stacking sequence of basal planes. Changes from one form to another often occur during crystal growth by vapor decomposition, producing variations in semiconductor properties. The SEM clearly shows the differences in

external form, and, with bias voltages applied to the crystal, reveals potential barriers developed at growth interfaces. Figure 19 provides an overall view of the whisker-size crystal containing external growth discontinuities; note especially the one just below the spherical tip (which is itself a growth defect). Figure 20 shows a closeup of this discontinuity, along with a discontinuity in another crystal which appears less faceted and more "lumpy."

A silicon carbide crystal with biasing electrodes attached is shown in figure 21. Figure 22 shows the same crystal with a bias of plus-80 volts applied to the right-hand contact. Figure 23 shows it with minus-80 volts. A barrier which reverses contrast and shifts position slightly with change in polarity is revealed by the light-dark contrast.

Another space-related application of the SEM is ascertaining the degree and type of damage caused by various types of synthetic micrometeorite bombardment to several potential protective-skin and structural materials. Figure 24 shows damage to an aluminum alloy by fine silicon carbide particles, and in figure 25 at lower magnification, damage to a stainless steel sample by larger hollow silica "microballoons" is shown.

The final example takes the form of a striking "abstract microsculpture." Figure 26 is a micrograph of chromium oxide crystal growths on a TD-Nichrome wire oxidized at 2200° F (1204° C) in air for 2 hours.

CONVENTIONAL ELECTRON MICROSCOPE

The conventional electron microscope (TEM) merits here a brief review of some of its characteristics and applications relative to the microprobe and SEM. It, of course, differs from the microprobe and SEM in having additional magnetic image-forming lenses and apertures below the sample. Typical incident-beam currents are much higher in the TEM - in the microampere range, contrasted to the nanoampere and picoampere-range beam currents typical of the probe and SEM, respectively. The static (nonscanning) beam must pass completely through the sample, which generally cannot be more than

0.1 to 0.2 micrometer thick, then must be focussed to form an image. The image-forming lenses may number from two to five, three being most common. They then are called objective, intermediate and projector lenses. The sample is positioned very close to or inside of the objective lens bore, and the image is projected onto a fluorescent screen which is tilted aside during photographic exposures. If one is examining directly an electron-transparent thin foil or section of a crystalline material, the image contrast of which results predominantly from diffraction effects, he must be able to tilt his sample during observation, to obtain suitable diffraction conditions. This is unnecessary with amorphous, replica, or biological specimens. A disadvantage, relative to the SEM, is that the photographic film or plates must be exposed and manipulated inside the vacuum.

Successful conventional electron microscopy of any sort depends on meticulous sample preparation, which often is difficult, sophisticated and tedious, and is indeed a fine art. In preparation of all types of specimens including thin foils, but especially of replicas, development in the sample which actually is examined in the TEM column of false features called artifacts often can result in completely misleading interpretations; these are a lesser problem with the SEM. The SEM therefore often is the better choice of instrument to use in many applications such as fractography. When unavoidable, artifacts must be recognized and discounted. This requires a high level of skill and experience, plus for crystals an understanding of diffraction phenomena. A diffraction pattern and its solution are required for almost every significant micrograph of most crystalline samples, for maximum yield of information. Solving a diffraction pattern may require tens of hours in a difficult case.

However, despite these drawbacks, this microscope remains our only commerically available instrument for observing features finer than 200 to 300 Angstroms (20 to 30 nm). It constitutes a very powerful tool for studying the fundamentals of such phenomena as plastic deformation and precipitation in solid crystalline materials, and for studying the substructural details of very fine grains, subgrains and twins; stacking faults; condensed vacancies and interstitial atoms; and domains of several types.

CONCLUDING REMARKS

This paper has described electron-optical metallographic instruments and techniques with two objectives: (1) To acquaint the materials technologist who has limited familiarity with the three major instruments with their important characteristics and their similarities and differences, and (2) To point out for the user of instrument service the capabilities and especially some limitations of the instruments and their performance. The microprobe has been emphasized because it is extremely versatile and useful, and because it incorporates many of the characteristics and operating modes of the other two instruments, plus its characteristic-X-ray-analysis capability.

REFERENCES

1. Kyser, D. F.; and Wittry, D. B.: Cathodoluminescence in Gallium Arsenide. The Electron Microprobe. T. D. McKinley, K. F. J. Heinrich, and D. B. Wittry, eds., John Wiley & Sons, Inc., 1966, pp. 691-714.

2. Dryer, H. T.: Modern Techniques of Microprobe Analysis. Presented at the Southwestern Symposium on Spectroscopy, Jan. 1966.

3. Lifshin, E.; and Hanneman, R. E.: Electron Microbeam Probe Analysis. Rep. 65-RL-3944M, General Electric Co., Apr. 1965.

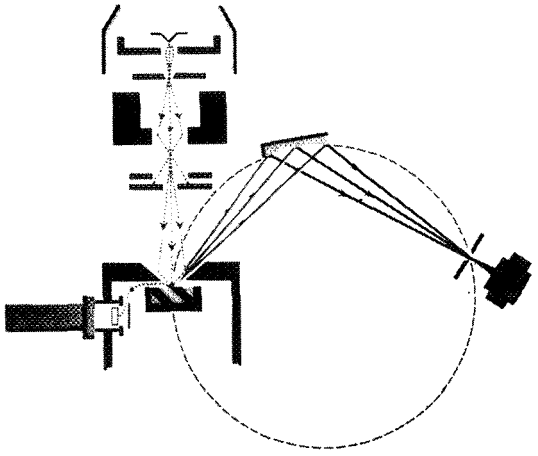

Figure 1. Simplified diagram of a microprobe with one crystal spectrometer and a secondary electron detector.

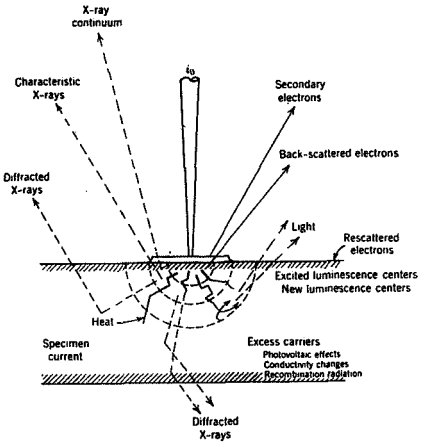

Figure 2. Physical processes that occur when an electron beam strikes a solid target. (Ref. 1)

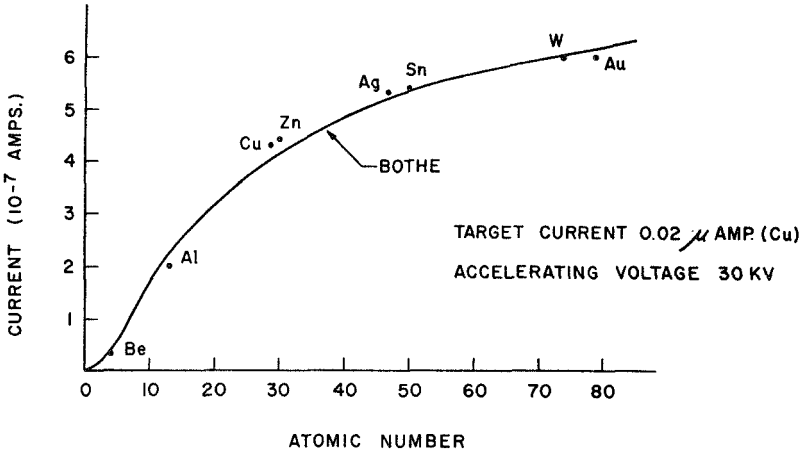

Figure 3. Output of backscattered electron detector as a function of atomic number. (Ref. 2)

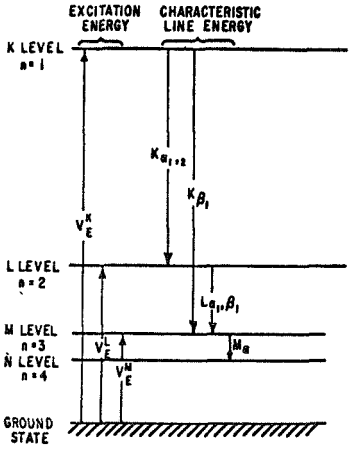

Figure 4. Schematic diagram of important transitions that cause emission of characteristic K, L, and M characteristic X-ray lines. (Ref. 3)

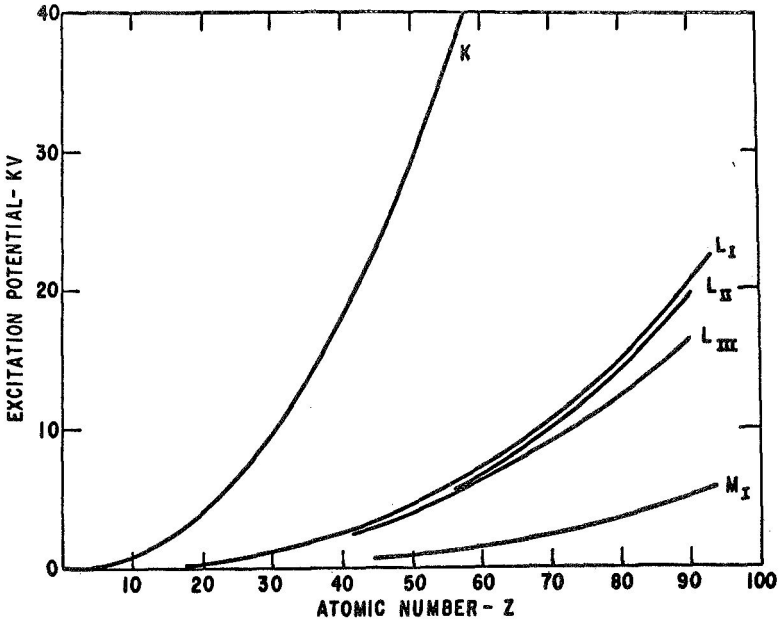

Figure 5. Minimum excitation energies of K, L and M x-ray spectral series as a function of atomic number. (Ref. 3)

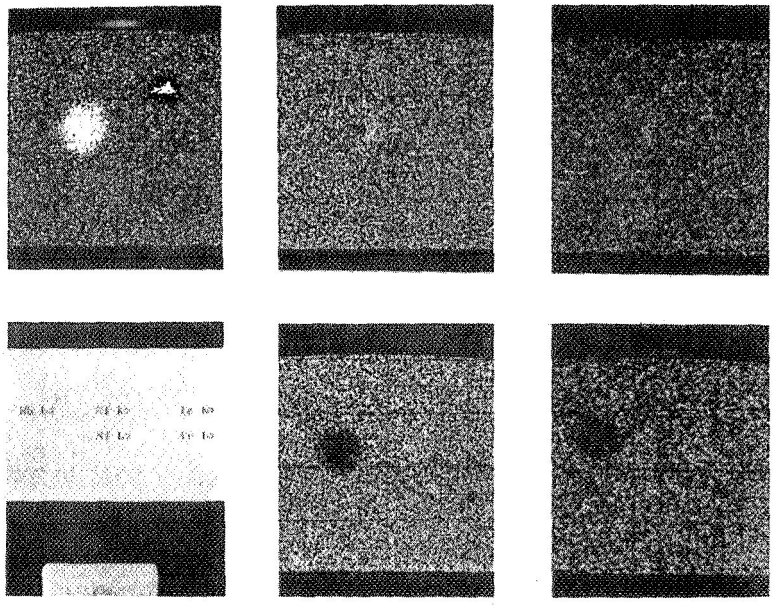

Figure 6. Effect of decreasing excitation potential on x-ray raster micrographs of thin Nb inclusion in a nickel steel. Top row: 20 kV, Nb-L-alpha, Ni-K-alpha, and Fe-K-alpha; bottom row: 5 kV, Ni-L-alpha, Fe-L-alpha. Approx. 600X. (Ref. 2)

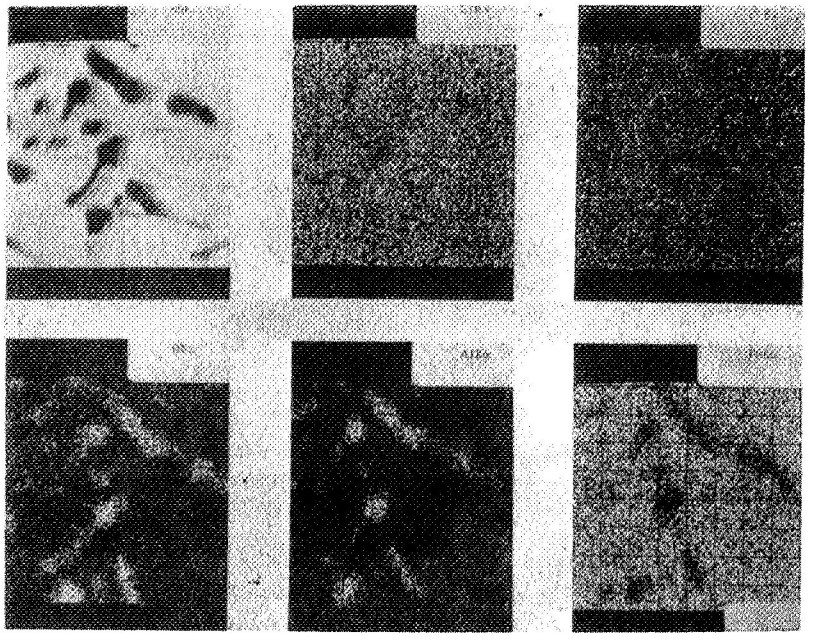

Figure 7. Backscattered-electron and x-ray raster micrographs of aluminum oxide inclusions in a nickel steel. Top row: 20 kV, back-scattered electrons, Ni-K-alpha, Fe-K-alpha; bottom row: 5 kV, O-K-alpha, Al-K-alpha, Fe-L-alpha. Approx. 600X. (Ref. 2)

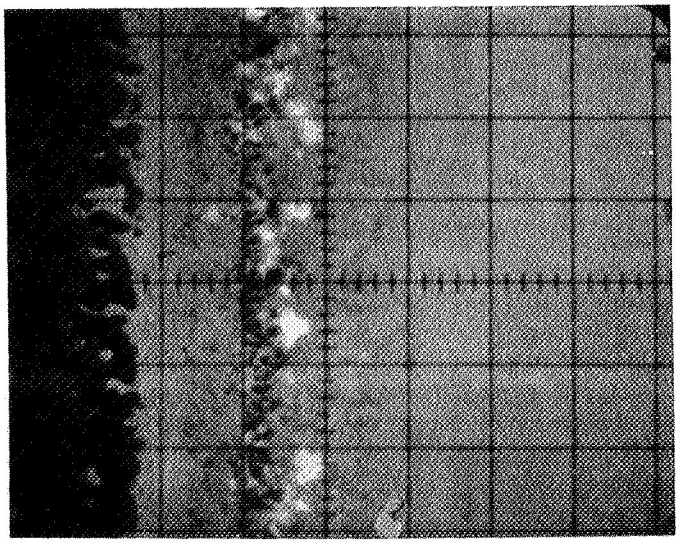

Figure 8. B.S.E. raster micrograph of oxidized Al-Cr-Fe protective coating on IN-100 nickel-base alloy, showing atomic-number sensitivity of this mode. Bright spots are thorium-containing artifacts. Approx. 250X.

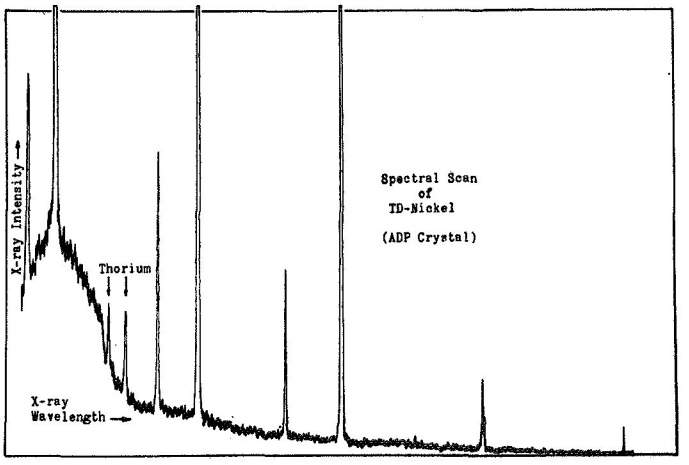

Figure 9. Spectral scan of TD-Nickel obtained using ADP crystal, showing two indicated peaks for Th (M-beta, 1st, and M-alpha, 1st), and nine Ni peaks (K-beta, 2nd through 5th orders and K-alpha, 2nd through 6th).

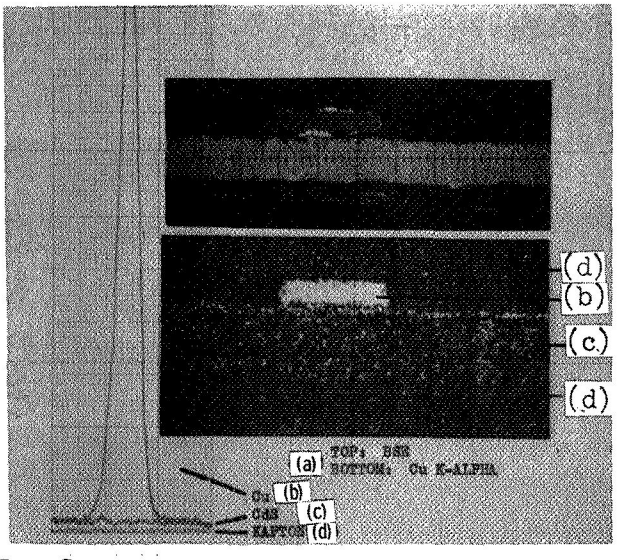

Figure 10. Copper x-ray raster micrograph of section through CdS solar cell showing in (a) top to bottom, layers as follows: Kapton, Cu_2S, CdS, Kapton, and including sections through gold-epoxy-coated copper grid wires. At left are shown spectral scans through the wavelength of Cu-K-alpha 1st-order peak obtained in (b) Cu grid, (c) CdS layer, and (d) Kapton plastic.

Approx.

450X.

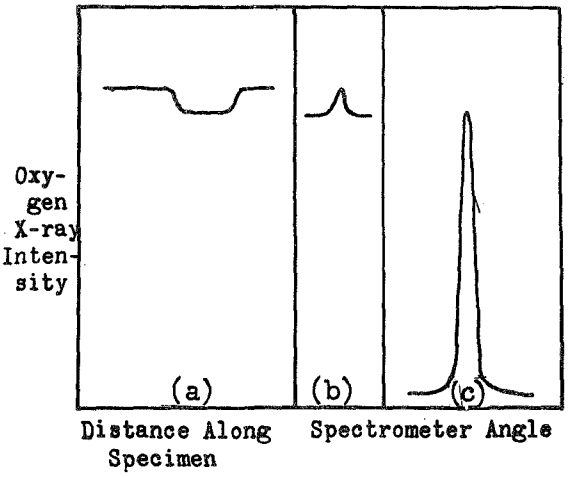

Figure 11. Sketch of (a) microprobe specimen traverse for oxygen across Al_2O_3 inclusion in steel; (b) oxygen x-ray spectral peak with electron beam on steel matrix showing very high background; and (c) oxygen x-ray spectral peak with beam on oxide inclusion, showing high peak and low background. High oxygen background on steel explains anomaly.

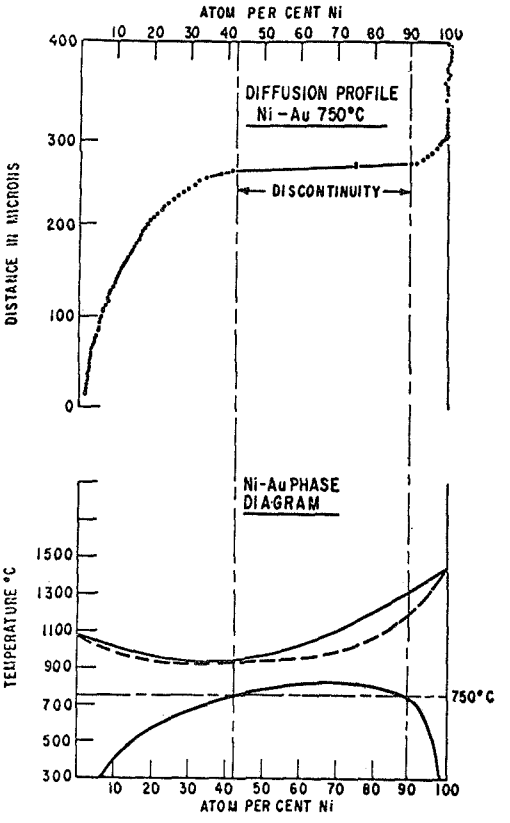

Figure 13. Step traverse of a gold-nickel diffusion couple after diffusion at 750°C showing concentration discontinuity corresponding to the two-phase region of the binary phase diagram at that temperature. (Ref. 3)

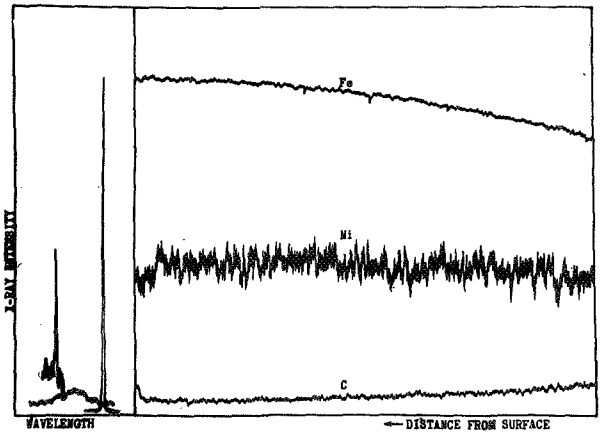

Figure 12. Continuous specimen traverse of transverse section through case of carburized AISI 4619 steel bar, showing (bottom to top) carbon, nickel and iron profiles. At left, spectral mini-scans through the three peaks used in specimen traverse, showing peak and background levels; left to right: Ni, C and Fe K-alpha, 1st order peaks. Distance covered by profiles is approximately 2000 microns (.080 inch).

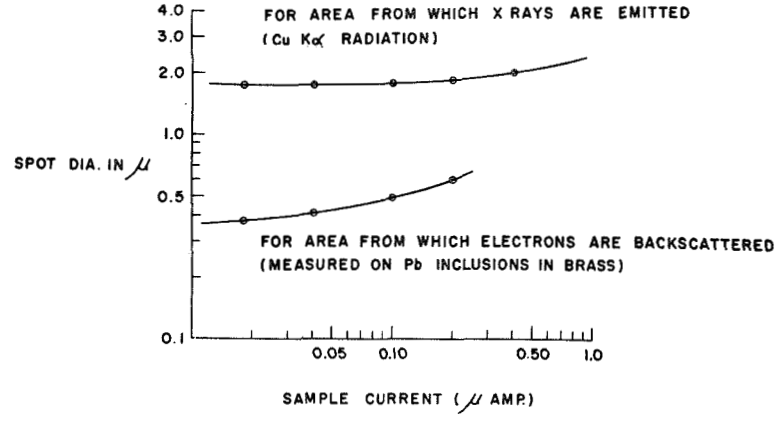

Figure 14. Typical back scatter-electron-emission and x-ray-emission spot sizes as a function of sample current for an electron microprobe. Accelerating voltage: 30kv (Ref. 2)

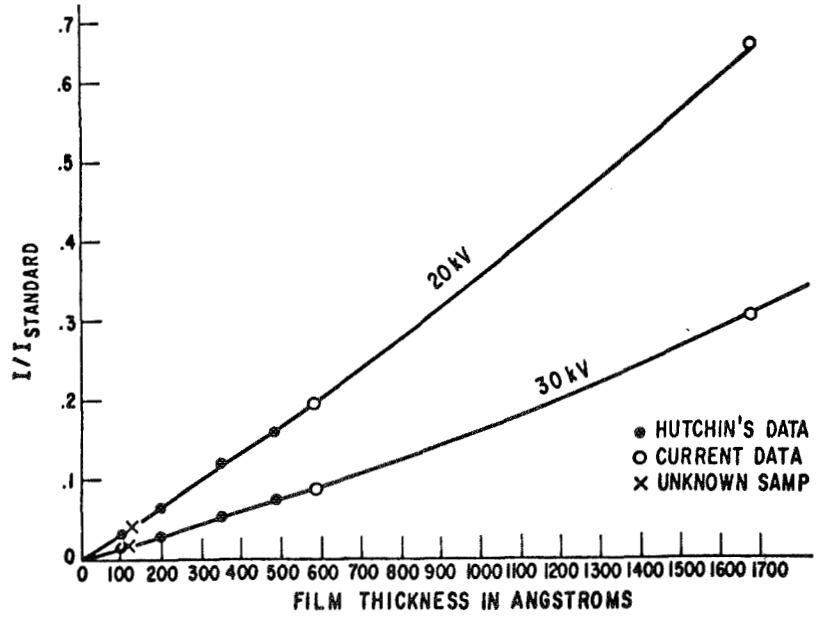

Figure 15. Calibration curves for thin-film thickness determination with the electron microprobe. Corrected relative intensity of Au-L-alpha x-rays vs. film thickness of gold on Si and SiO_2 substrates. (Ref. 3)

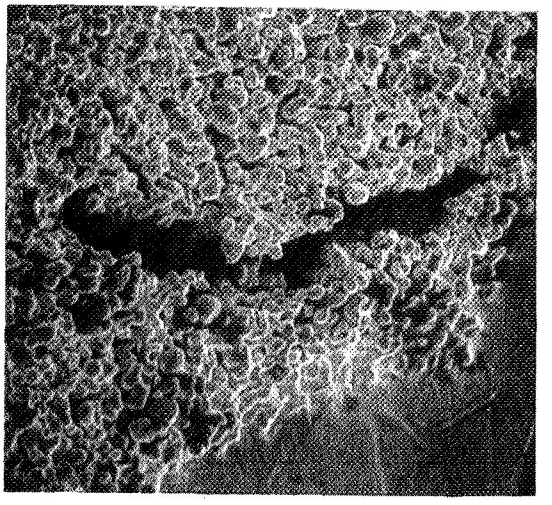

Figure 16. Defective region in porous tungsten "mercury vaporizer" of Sert-II ion thruster. SEM 750X.

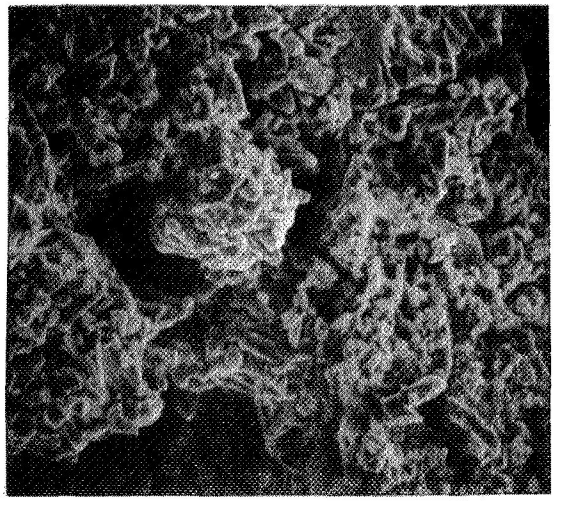

Figure 17. Fracture of complex sodium-manganese titanate, pressed and sintered, showing characterization of a material too friable to permit preparation of polished section. SEM, approx. 400X.

Figure 18. Widmanstatten structure developed by relatively deep etching in an NiAl coating on IN-100 alloy which had been oxidized in static air at 2000°F for 300 hr., then reheated and slow cooled. Etchant: HCl, Hn HCl, HNO_3, wateringlycerin, electrolytic, 3·· volts. SEM, approx. 1800X.

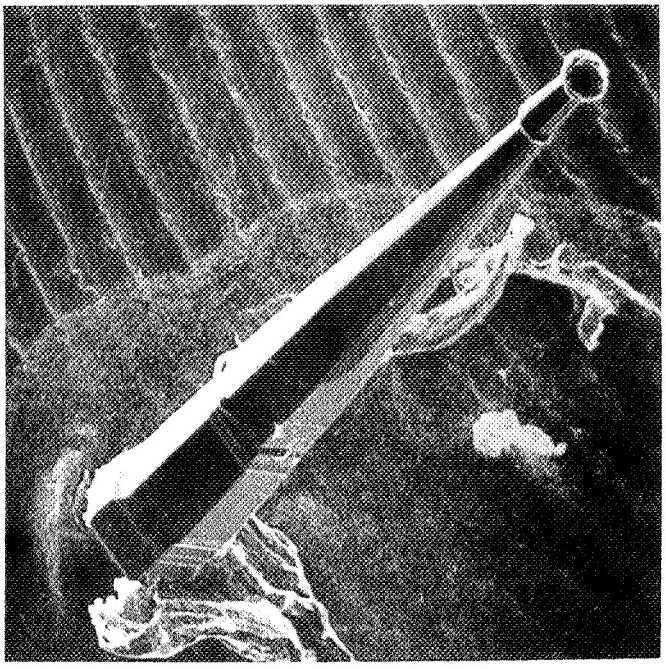

Figure 19. Single silicon carbide semiconductor crystal containing several growth discontinuities including spherical termination. SEM, approx. 100X.

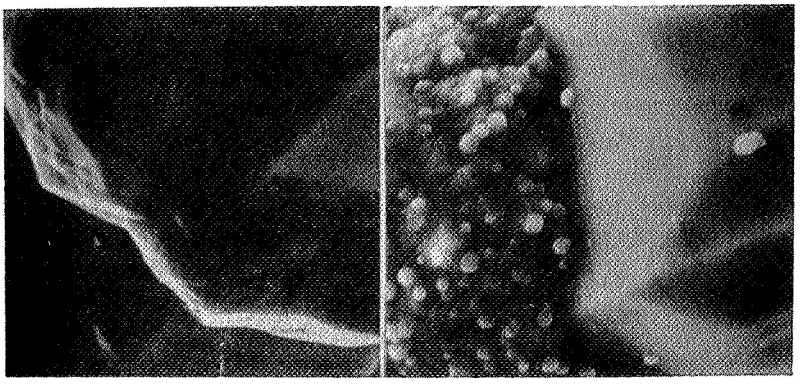

Figure 20 Close-up of mostly-faceted growth discontinuity just below termination, in SiC crystal of Figure 19, and in another crystal a non-faceted (botryoidal) growth discontinuity. SEM, approx. 1200X.

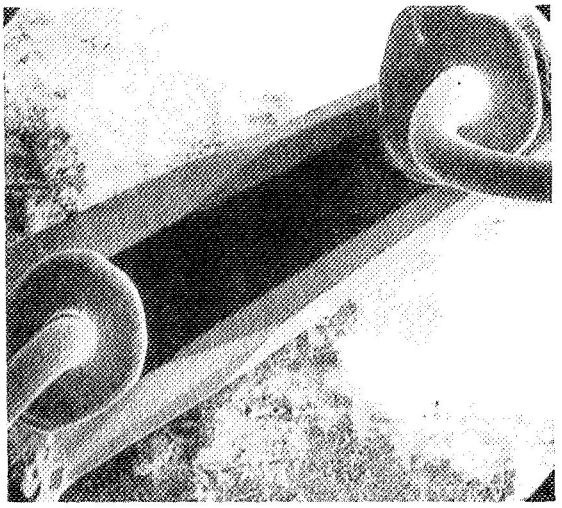

Figure 21 Silicon carbide semiconductor crystal with biasing electrodes attached, unbiased. SEM, approx. 120X.

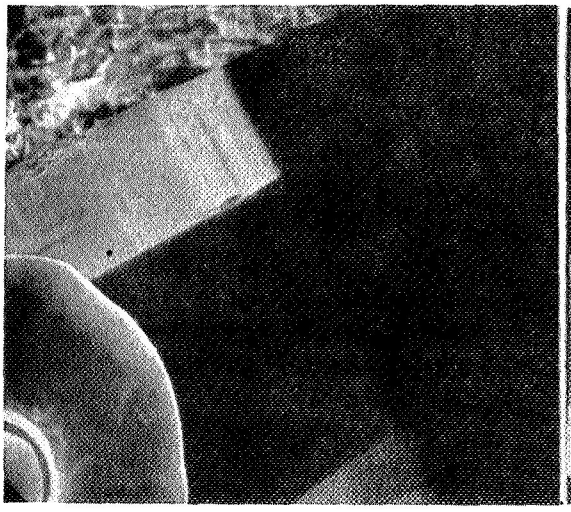

Figure 22 Crystal of Figure 20 with plus-80 volts bias on right-hand electrode, showing development of intense barrier revealed by light-dark contrast. SEM, approx. 300X.

Figure 23. Same as Figure 21, but with 80-volt bias reversed (minus 80 volts on right-hand electrode). Note less-intense reversed barrier, in a slightly different position. SEM, approx. 300X.

Figure 24 Simulated micrometeorite damage in aluminum alloy bombarded with angular silicon-carbide particles. SEM, approx. 150OX.

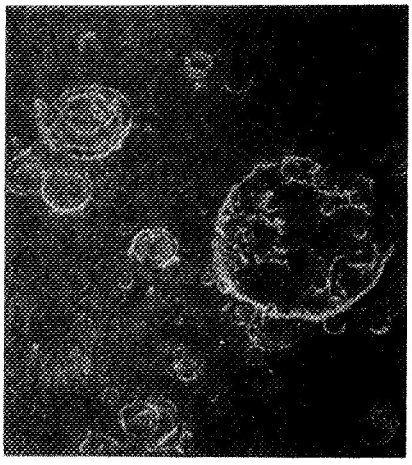

Figure 25 Simulated micrometeorite damage in stainless steel bombarded by hollow silica "microballoons". SEM, approx. 100X.

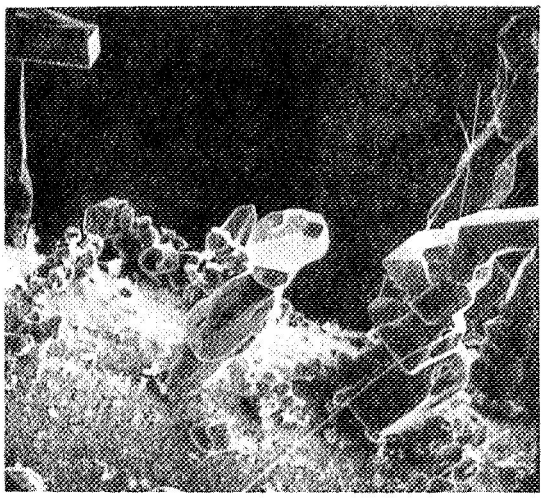

Figure 26 "Abstract sculpture" micrograph: Cr_2O_3 crystals on TD-Nichrome wire oxidized in air at 2200°F (1205°C) for 2 hours. SEM, approx. 450X.